Study for Mechanism of Fatigue Crack Propagation by Measuring Slip Amount at Crack Tip

HIROYUKI MASUDA, SABURO MATSUOKA and SATOSHI NISHIJIMA

National Research Institute for Metals, 2–3–12, Nakameguro, Meguro-ku, Tokyo, Japan, 153

Abstract

In order to understand the mechanism of fatigue crack propagation in steels with different yield strength, the amount of slip at the crack tip was measured under the monotonic and cyclic loading conditions by the step loading method. The results show that the amount of slip at the crack tip is in accordance with that predicted from the theory obtained under monotonic loading conditions. However the amount of slip at the crack tip under cyclic loading conditions is very small and is nearly equal to the amount of crack growth in one cycle of the loading process. This sudden decrease in the amount of slip at the crack tip under the cyclic loading condition can be explained by assuming the existence of a thin ideal strength phase near the crack tip.

Keywords

Fatigue crack growth, Stretch zone width, Step loading, Fractography, Ideal strength

Introduction

Although the slip amount at the crack tip is the rate controlling factor for crack propagation and is important for understanding the mechanism of fatigue, there have been few reports measuring this amount. One of the reasons is that these measurements are difficult. However as the personal computer has become developed, controlled K-value step loading tests have become easier.

In this paper, in order to understand the mechanism of fatigue crack propagation, various controlled K-value step loading tests were carried out for steels with different yield strength and the slip amount at the crack tip was measured by a fractographic method. In addition, the factors which control the slip amount are discussed.

Experimental Method

The test materials used were SUS304 stainless steel, SUS329J1 duplex stainless steel, SM50B steel and SNCM439 high strength steel (tempered at 600° C). The chemical composition and the mechanical properties of test materials are given in Table 1. Fatigue tests were performed on compact tension type specimens of 50 mm width in the air at room temperature. The test frequencies used were from 2 to 30 Hz. The tests were performed by using the computer system (Masuda et al., 1986), and the crack length and the crack closure level were derived from calculating the elastic compliance. The crack propagation test employed was a maximum constant load ΔK-decreasing method (R = 0.3~0.9) when $\Delta K \leqq 10$ MPa·m$^{1/2}$ and a constant stress ratio (R = 0.3, 0.5) ΔK-increasing method when $\Delta K \geqq 10$ MPa·m$^{1/2}$ for the purpose of preventing crack closure. The slip trace at the crack tip was produced by using four types of step loading test as shown in Figure 1(a)~(d), where ΔK was kept constant except when the mean load was changed. After the fatigue tests were finished, the slip amount at the crack tip was measured by a fractographic method.

Experimental Results

Crack Propagation Properties

Fig.2 shows the the crack propagation curves for various alloys. The crack propagation curves are similar to each other and independent of the yield strength of the alloys. It is notable that the crack propagation rate is proportional to ΔK^2 when $\Delta K \geqq 30$ MPa·m$^{1/2}$.

Slip Amount at Crack Tip

In order to measure the slip amount at the crack tip, the test method shown in Fig.1(a) was used. In this method, care was taken to ensure that the reverse slip during unloading was kept to a minimum. Therefore ΔK = 5 MPa·m$^{1/2}$ was used for the crack propagation. In addition, fatigue tests were carried out under the condition that $K_{min} \geqq 5$ MPa·m$^{1/2}$ for the purpose of preventing crack closure. An influence of the value of K_{min} on the slip amount was not observed. The effect of yield strength on the slip amount was first studied for all alloys shown in Table 1 under the condition that the amount of K-mean change ΔK_h = 28 MPa·m$^{1/2}$. Fig.3 shows the slip trace (stretch zone) on the fracture surface of two alloys with different yield strength, where the photo was taken with a tilt angle of 45° to the crack plane. It is generally observed that the stretch zone has the angle of 50~70° to the crack plane. Fig.4 shows the relation between its width (stretch zone width hereafter SZW) and yield strength σ_y. There is a tendency for the SZW to become bigger as the yield strength decreases and SZW is given by the equation (1):

$$SZW \fallingdotseq \Delta K_h^2 / 2\sigma_y E \qquad (1)$$

where E is Young's modulus and is 2 x 10^5 MPa for iron.

Table 1 Chemical and mechanical properties of materials

Material	C	Si	Mn	P	S	Ni	Cr	Mo	Cu	σy(MPa)	σB(MPa)
SUS304	0.06	0.53	1.11	0.039	0.010	9.04	18.3	-	-	336	629
SUS329J1	0.02	0.58	0.68	0.013	-	5.80	24.9	2.35	0.01	549	705
SM50B	0.15	0.37	1.36	0.020	0.005	0.03	0.02	-	0.01	372	530
SNCM439	0.40	0.33	0.77	0.008	0.004	1.88	0.88	0.26	0.02	974	1083

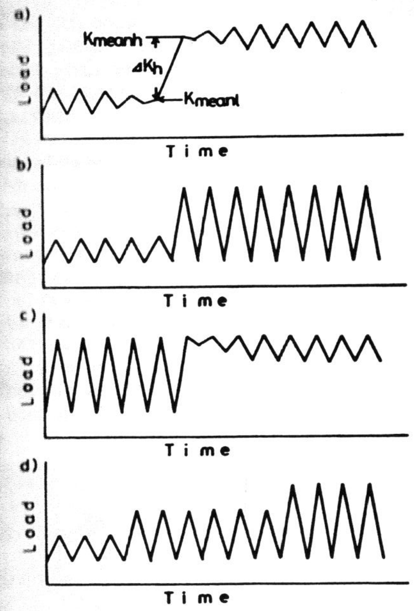

Fig.1 Various test method.

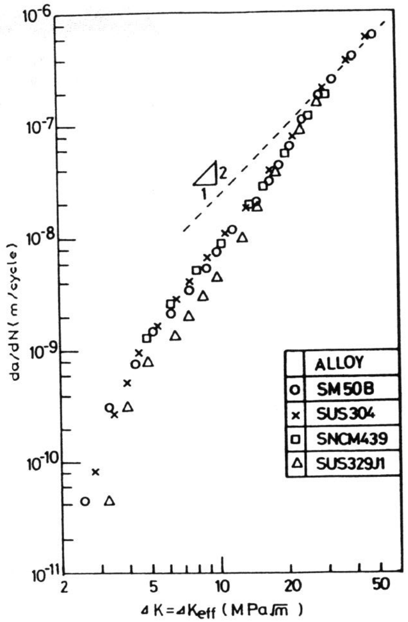

Fig.2 da/dN vs. ΔK curves for various alloys.

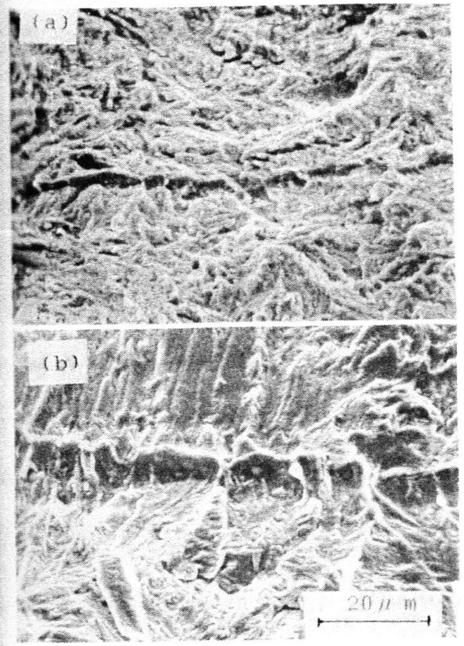

Fig.3 Slip trace on fracture ← surface. (a)SNCM439 and (b)SUS304. ΔK_h = 28 MPa·m$^{1/2}$

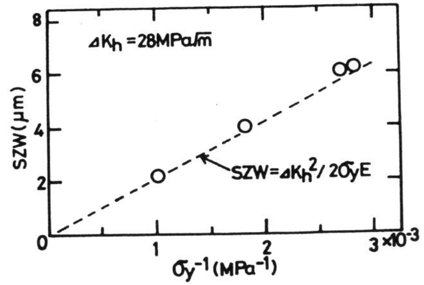

Fig.4 Relation between SZW and σ_y

The influence of ΔK_h on SZW was studied with the test method shown in Fig.1(a) for various ΔK_h values. SUS329J1 stainless steel was used in this experiment, because the observation of the SZW is the easiest among the tested alloys. Fig.5 shows the stretch zone produced under various ΔK_h conditions. The SZW is dependent on ΔK_h as shown in Fig.6 and is expressed by eq.(1).

On the test method shown in Fig.1(a), both K_{max} and K_{min} were changed. In order to study the influence of test method on SZW two different types of test were performed. One is that where K_{min} is kept constant and only K_{max} is changed as shown in Fig.1(b). The other is where K_{max} is kept constant and only K_{min} is changed as shown in Fig.1(c). The SZW observed by the test method shown in Fig.1(c) corresponds to the slip amount produced at the crack tip during propagation. Fig.7 shows the stretch zone for SUS304 stainless steel produced by the test method shown in Fig.1(b) where ΔK is changed 10 →40 $MPa\cdot m^{1/2}$. It is surprising that in spite of some reversed slip having occurred during the unloading process, a large stretch zone with an angle of 50~70° with respect to the crack plane was observed on the fracture surface. While in the case of the test carried out using the method shown in Fig.1(c), the SZW was very small and was independent of the test

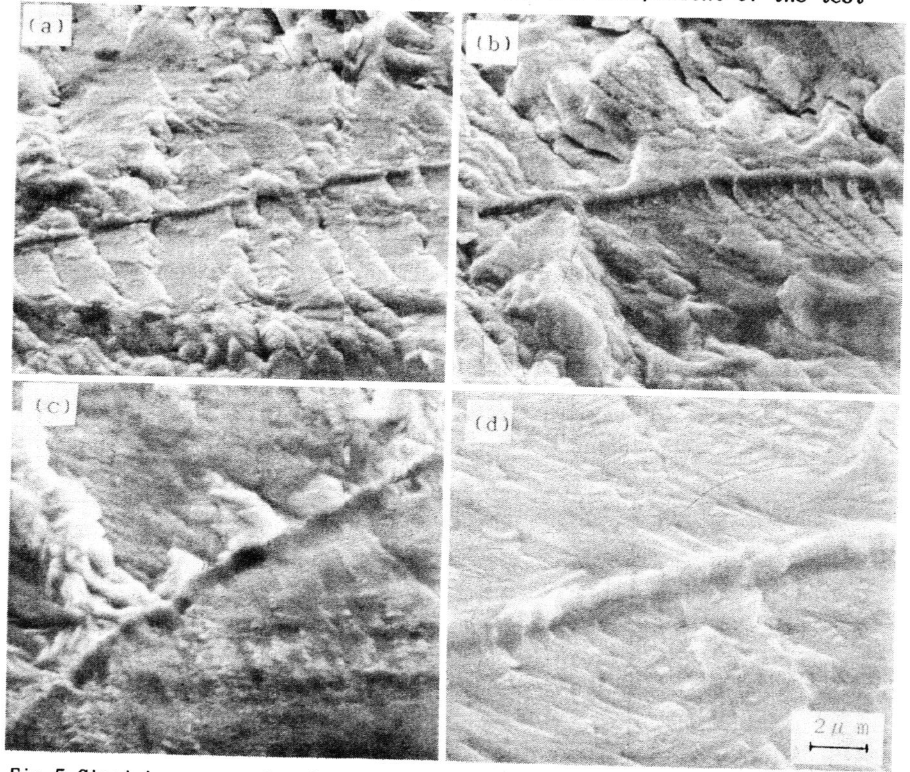

Fig.5 Stretch zone produced under various ΔKh.
(a)ΔKh= 6 MPa·√m,(b)ΔKh= 9 MPa·√m,
(c)ΔKh= 12 MPa·√m and (d)ΔKh= 15 MPa·√m.

materials used being nearly equal to the crack growth in one cycle of the loading process. Fig.8 shows the stretch zone for SUS304 stainless produced by the test method shown in Fig.1(c) where ΔK is changed 40 → 5 $MPa\cdot m^{1/2}$. A two step loading test shown in Fig.1(d) was performed for the purpose of checking the amount of reverse slip occurring during unloading on the test method shown in Fig.1(b). In this test the material used was SUS304 stainless steel and ΔK was changed 20 → 40→ 50 $MPa\cdot m^{1/2}$. Two stretch zones corresponding to the load change are observed on the fracture surface as shown in Fig.9. In addition to these two big stretch zones, the numbers of striations produced by cycling at ΔK = 40 $MPa\cdot m^{1/2}$ corresponds to the number of loading cycles (6) imposed at the first load change as shown schematically in Fig.10. From this it is evident that the crack was produced during unloading by the reverse slip and that comparing to the amount of slip during loading, the amount of reverse slip during unloading is very small.

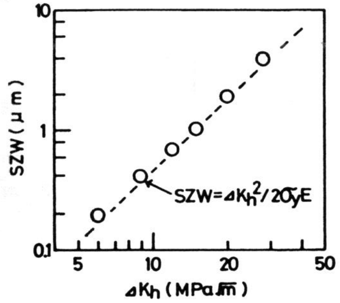

Fig.6 SZW vs. ΔK_h

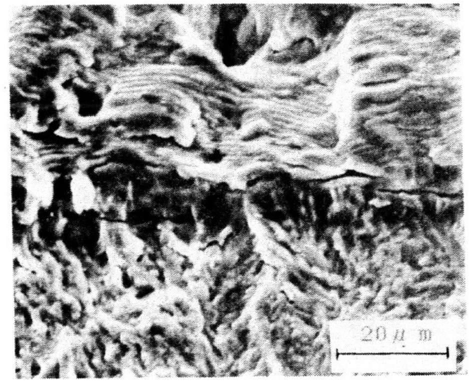

Fig.7 Stretch zone produced by Fig.1(b) method

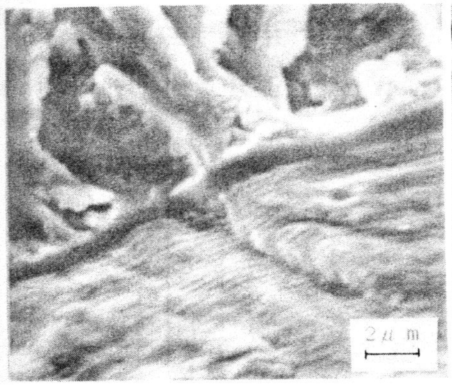

Fig.8 Stretch zone produced by Fig.1(c) method.

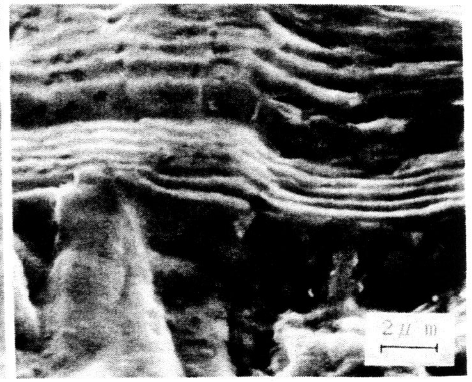

Fig.9 Stretch zone produced by Fig.1(d) method.

Discussion

Mechanism of Crack Propagation

Considering from the observation in SEM by Neumann (1974) and Kikukawa et al. (1978), the mechanism of the crack propagation seems to be that shown in Fig.11: as the load increases the alternating slip occurs at the crack tip, the crack opens and the chemical reaction proceeds at the bare surface. During unloading the reversal alternating slip occurs. The slip plane where no chemical reaction has taken place rewelds but not for the plane where the chemical reaction has taken place. As the results, the crack propagates.

If we assume the angle between the crack plane and slip plane is about 60°, the amount of the crack growth becomes nearly equal to the SZW under the condition where no rewelding of the slip plane occurs. This corresponds with the observation as shown in Fig.8. According to this mechanism the crack opening starts at $\Delta K = 0$ and the crack propagation rate must be proportional to ΔK^2. Among the tested ΔK regions this relation is satisfied only when $\Delta K \geqq 30$ MPa·$m^{1/2}$ as shown in Fig.2. The hesitation of the crack growth by the grain boundary at low ΔK regions is considered as the reason, however the proof of it is the future work.

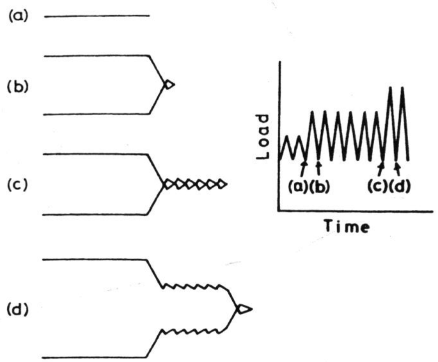

Fig.10 Crack propagation mechanism at two step loading.

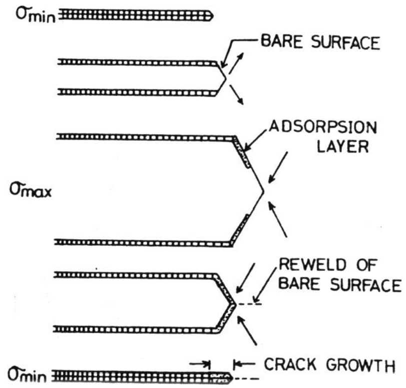

Fig.11 Crack propagation model.

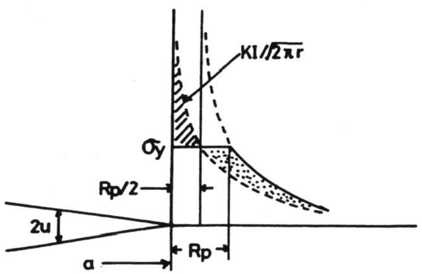

Fig.12 Model of stress distribution at crack tip.

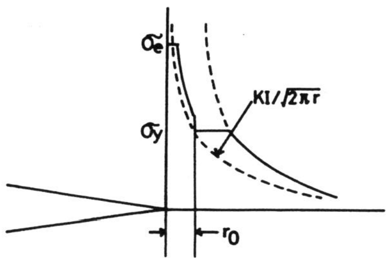

Fig.13 Stress distribution model for two phase material.

Slip Amount at Crack Tip

If we regard the material is a perfect elastic-plastic body, the stress distribution on the extension line of the crack tip σ_x, σ_y and the displacement at the crack plane u as shown in Fig.12 are given by eq.(2) and (3) respectively (Irwin, 1957):

$$\sigma_x = \sigma_y = K_I/(2\pi r)^{1/2} \qquad (2)$$

$$u = (\kappa+1)K_I(r/2\pi)^{1/2}/2G \qquad (3)$$

where r is the distance from the crack tip, κ is the constant and G is the modulus of rigidity. However since materials yield near the crack tip, the stress distribution near the crack tip is considered to be that shown by a solid line. From the view point of energy balance: the area shown by an oblique line is equal to that shown by a dot line, the plastic zone size $R_p = (K_I/\sigma_y)^2/\pi$ can be obtained. Then using the stress distribution where the crack tip locates as if it were $a + R_p/2$, the crack tip opening displacement (CTOD) is given by eq.(4):

$$CTOD = 2u = (\kappa+1)K_I(R_p/4\pi)^{1/2}/G$$

$$= 4K_I^2/\pi\sigma_y E \qquad \text{(plane stress)}$$

$$= 4(1-\nu^2)K_I^2/\pi\sigma_y \qquad \text{(plane strain)} \qquad (4)$$

where a is the crack length, ν is Poisson's ratio and usually 1/3. It is apparent from the experimental results that ΔK_h is one of the controlling factors for the amount of slip at the crack tip. Assuming that the angle between the crack plane and the stretch zone is 65° and that the effective ΔK is equal to ΔK_h: the crack opening starts at $K = K_{meanI}$, the SZW measured from the photo is considered to be nearly equal to CTOD/2. As the tests were done under the plane strain condition, the SZW is expressed by eq.(5):

$$SZW \fallingdotseq CTOD/2 = 0.57\Delta K_h^2/\sigma_y E \qquad (5)$$

there is a good coincidence between the theoretical value and the experimental results. Thus the slip behavior under the monotonic loading condition was found to obey the theory. While according to Rice (1967), the amount of slip at the crack tip and plastic zone size under the cyclic loading condi

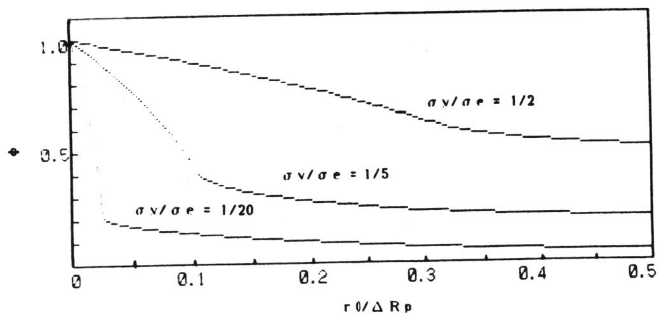

Fig.14 CTOD ratio (Φ) as a function of r0/ΔRp and σy/σe

tion is given by substituting σ_y to $2\sigma_y$:

$$SZW \fallingdotseq CTOD/2=0.28\Delta K^2/\sigma_y E \qquad (6)$$

$$\Delta R_p=R_p/4=(\Delta K/\sigma_y)^2/4\pi \qquad (7)$$

However the amount of slip predicted from the theory is completely different from that observed on the test method shown in Fig.1(a): the amount of slip at the crack tip during loading is very small and nearly equal to the crack growth in one cycle of loading process. The slip behavior observed on the two step loading tests shows that the amount of slip during unloading (reverse slip) became much smaller than that during loading. These sudden decrease in the amount of slip at the crack tip is considered to be due to the increase of the yield strength of the materials near the crack tip.

Therefore the amount of slip on the duplex phase material with the yield strength of σ_y and σ_e is considered. From the view point of energy balance, the stress distribution shown in Fig.13 is considered. Fig.14 shows the result of the analysis for the amount of slip at the crack tip on the two phase material where r_0 is the width of the phase with the yield strength of σ_e and Φ is the ratio of CTOD for the duplex phase material to that for the single phase material with the yield strength of σ_y. Since ΔR_p is a function of ΔK, $r_0/\Delta R_p$ closes to 0 as ΔK increases if r_0 is assumed constant. It is apparent from the figure that the amount of slip increases rapidly and approaches to that on the single phase material when $r_0/\Delta R_p<\sigma_y/2\sigma_e$.

Considering from the sudden increase in the amount of slip when K_{mean} is increased, r_0 at maximum loading during the cyclic loading seems to close to $\Delta R_p \sigma_y/2\sigma_e$. From the analysis, σ_e is supposed to be nearly equal to the ideal strength of E/10. For example calculating from eq.(6) the SZW at ΔK = 30 MPa$\cdot$m$^{1/2}$ for SNCM439 steel is 1.3μm. since σ_y/σ_e is about 1/20 and Φ is 0.16~0.2 around $r_0 \fallingdotseq \Delta R_p \sigma_y/2\sigma_e$(=1.8$\mu$m), we have the SZW of 0.21~0.26μm during the crack propagation which is in accordance with the experimental results. The possibility of the existence of high strength phase is high, however the proof of it is the future work.

Conclusion

The amount of slip at the crack tip under the monotonic loading condition was found to obey the theory. However the amount of slip at the crack tip under the cyclic loading condition was small and nearly equal to the crack growth in one cycle of loading process and not in accordance with the theory. These sudden decrease in the amount of slip at the crack tip under the cyclic loading condition can be explained by assuming the existence of a thin high strength phase near the crack tip.

References

Masuda,H., Matuoka,S., Nishijima,S., and Shimodaira,M.,(1986), Boushokugijutu, 35, 27-34

Neumann,P., (1974). Acta.Met., 22, 1157-1162

Kikukawa,M., Jono,M., and Adachi,M., (1978), Zairyo, 27, 39-44

Irwin,G.R. (1957), J.Apl. Mech., 24, 361-364

Rice,J.R.,(1967), ASTM STP 415, 247-309